JOURNAL OF CHEMICAL & ENGINEERING DATA

ARTICLE

pubs.acs.org/jced

Volumetric Adsorption Measurements of N_2, CO_2, CH_4, and a CO_2 + CH_4 Mixture on a Natural Chabazite from (5 to 3000) kPa

Guillaume C. Watson,[†] Nathan K. Jensen,[†] Thomas E. Rufford,[†] K. Ida Chan,[‡] and Eric F. May*[,†]

[†]Centre for Energy, School of Mechanical & Chemical Engineering, The University of Western Australia, Crawley, WA, Australia 6009

[‡]Chevron Energy Technology Company, Houston, Texas 77002, United States

ABSTRACT: We report here measured adsorption capacities for a natural chabazite zeolite at pressures ranging from (5 to 3000) kPa, at temperatures of (244 and 305) K, for pure N_2, CH_4, and CO_2, and for gas mixtures of CH_4 + CO_2. The pure gas data sets from this work and from the literature were in good agreement (10 %) and were regressed to Toth models over a wide range of pressure and temperature. We show that extrapolation of models that were fit only to low pressure data (below 120 kPa) can lead to a 30 % deviation in adsorption capacities predicted at high pressures. Similarly, models fit only to high pressure pure fluid data resulted in unreliable predictions for mixture adsorption capacities particularly when the component's partial pressure was low. The experimental results indicate that, while the chabazite is unlikely to be useful for N_2/CH_4 separation, it may have potential for removing bulk CO_2 from natural gas, particularly at low temperatures. A feed gas mixture of $0.95CH_4 + 0.05CO_2$ placed in contact with the chabazite resulted in equilibrium vapor phases with CO_2 mole fractions of about (0.0013 and 0.0002) at (305 and 244) K, respectively. The ideal adsorbed solution theory was used to successfully describe the observed mixture behavior, although it was found to be sensitive to the data range over which the pure fluid models were regressed.

INTRODUCTION

In 2009, natural gas (NG) supplied 24.2 % of the global energy demand,[1] and that fraction is predicted to continue to grow because NG is the cleanest fossil fuel available for the generation of electricity. Many large markets for NG are located far from the reservoirs that supply them, and so large quantities of NG must be transported either by gas pipeline or, for most trans-continental trade, in tankers as liquefied natural gas (LNG). Of the impurities that must be removed from the NG to meet specifications for gas pipelines or the LNG plant feed, carbon dioxide and nitrogen are two of the most common and problematic.[2,3] For gas fields that contain high concentrations of N_2 and/or CO_2, the removal of these contaminants to meet LNG plant specifications (N_2 < 4 % vol, CO_2 < 50 ppmv)[2] can add significantly to gas production costs. The conventional technology employed for the removal of CO_2 from NG is absorption by aqueous amine solvents. This is an energy-intensive process with high capital costs and high operating costs, and the typical amine solvents present environmental or safety concerns. Nitrogen rejection is usually performed by cryogenic distillation. However, the capital and operating costs of cryogenic distillation plants are high, and this technology is not economically viable for gas feed rates below 15 MMscfd.[4]

Pressure swing adsorption (PSA) is a promising alternative technology for CO_2 and N_2 removal from NG because PSA processes have much lower energy requirements than amine-scrubbers and cryogenic distillation units.[5,6] Furthermore, the low-temperature and high-pressure conditions available in a LNG plant provide opportunities to enhance the efficacy of PSA processes for the separation of N_2, CO_2, and CH_4.[7−9] The identification of suitable adsorbents with high equilibrium capacities for CO_2 and N_2 is a key challenge to be overcome in the development of PSA processes for CO_2 and N_2 removal from NG. Central to this search for suitable adsorbents is the requirement for better data on the sorption behavior in gas mixtures, particularly at conditions (low temperature, high pressure) similar to those available in the LNG plant. This paper reports new data for a natural zeolite, chabazite, and evaluates it as a potential adsorbent for removing CO_2 and/or N_2 from NG by PSA.

The adsorption and separation of CO_2, N_2 and CH_4 has been studied on a large number of porous materials including activated carbons,[10−13] carbon molecular sieves,[14−16] and zeolites.[17−20] As a consequence of their crystalline structure, zeolites have narrow pore openings and a uniform pore size distribution and thus show great potential for the separation of small gas molecules (based on either kinetic or equilibrium selectivity). Synthetic zeolites such as 13X and 5A are among the most commonly used adsorbents in industrial gas separations,[13,15] but several naturally occurring zeolites including clinoptilolite, mordenite, and chabazite have pore structures and chemistry that may also be suitable for the separation of CO_2 and N_2 from NG.[21] Natural and modified versions of clinoptilolite (ion-exchange, thermal treatment, and structural change) have been used for upgrading and purification of natural gas, coal, and landfill gas.[21−23] In contrast, there are limited data at industrially relevant conditions (high pressure, gas mixtures) published in the open literature regarding the adsorption and separation of CO_2, N_2, and CH_4 on/using chabazite.

Chabazite (structural formula $(Ca_2, Na_4, K_4)[(AlO_2)_4(SiO_2)_8]\cdot 13H_2O$) has a three-dimensional framework delimited by eight-membered rings that create small pore openings (aperture 3.8 × 3.8 Å and kinetic pore diameter of 4.3 Å).[24] This structure

Received: July 28, 2011
Accepted: October 30, 2011
Published: November 28, 2011

suggests chabazite could be a selective adsorbent for CO_2 and/or N_2 from NG (kinetic diameter of molecules: CH_4 3.80 Å, N_2 3.64 Å, and CO_2 3.30 Å).[3] Chabazite, and (K, Na, Li, Mg, Ca, Ba) ion-exchanged versions of chabazite, have been used in adsorption-based processes for air purification and CO_2 capture from combustion flue gases by Webley and co-workers.[25−27] Also, in patents assigned to Air Products and Chemicals,[28−30] Coe and coauthors report the adsorption of N_2, Ar, CF_4, and O_2 on natural and (Ca, Sr, Li) ion-exchanged chabazites. They found that chabazites with a Si/Al ratio of 1.8 to 2.7 and an optimized divalent cation distribution throughout the framework showed improved adsorption properties over any other zeolites for weakly interacting adsorbates such as N_2.[29]

Previously we reported the use of a volumetric-type adsorption system for the measurement of the equilibrium adsorption capacity of pure N_2, CO_2 and CH_4 on a carbon molecular sieve at temperatures between (115 and 323) K and at pressures up to 5 MPa.[31] In this work we report the extension of this apparatus to measure the adsorption of gas mixtures over this range of temperature and pressure and thus to determine the uptake of individual gas components on an adsorbent. The use of the modified adsorption system is demonstrated with adsorption measurements of CH_4, CO_2, N_2, and a CH_4 + CO_2 mixture on chabazite at pressures from (5 to 3000) kPa and at temperatures of (244 and 305) K.

MATERIALS

Sodium chabazite from the Bowie deposit (Arizona, USA) was obtained from Zeox Corporation, formerly GSA Resources. Chabazite from this deposit has been reported to also contain other zeolite phases such as clinoptilolite and erionite,[32] impurities which could be removed by a chemical treatment in an alkaline-silicate medium. However, as purification treatments for natural zeolites can add prohibitive costs to their industrial application, we evaluated the gas separation performance of the unpurified natural chabazite. The as-received chabazite granules were simply sieved, and the 2 mm size fraction was used for the adsorption measurements.

The chemical composition and physical properties of the chabazite were characterized by powder X-ray diffraction (XRD), X-ray fluorescence spectroscopy, and He pycnometry. Pore structure and surface areas were determined from sorption analyses of N_2 at 77 K and CO_2 at 273 K. From the 77 K N_2 sorption analyses the chabazite sample's BET specific surface area was determined to be 415 $m^2 \cdot g^{-1}$, and the pore volume was determined to be 0.348 $cm^3 \cdot g^{-1}$. Jensen et al.[33] reported additional details about these characterizations together with the results of pure fluid adsorption uptake measurements at low pressures, (0.001 to 120) kPa, at (248, 273 and 302) K made with a commercial ASAP2020 apparatus (Micromeritics, USA).[34] These low-pressure measurements were important to the current work because they provided a benchmark for the high-pressure pure fluid measurements reported here, and they were essential to the interpretation of the high-pressure mixture measurements when the partial pressure of the CO_2 in the vapor phase was very low.

All gases used in this work were supplied by BOC who stated the following mole fraction purities: He 0.99999, Ar 0.99999, CH_4 0.99995, N_2 0.99999, and CO_2 0.9999. The estimated uncertainty of the adsorption measurements due to gas purity is negligible.

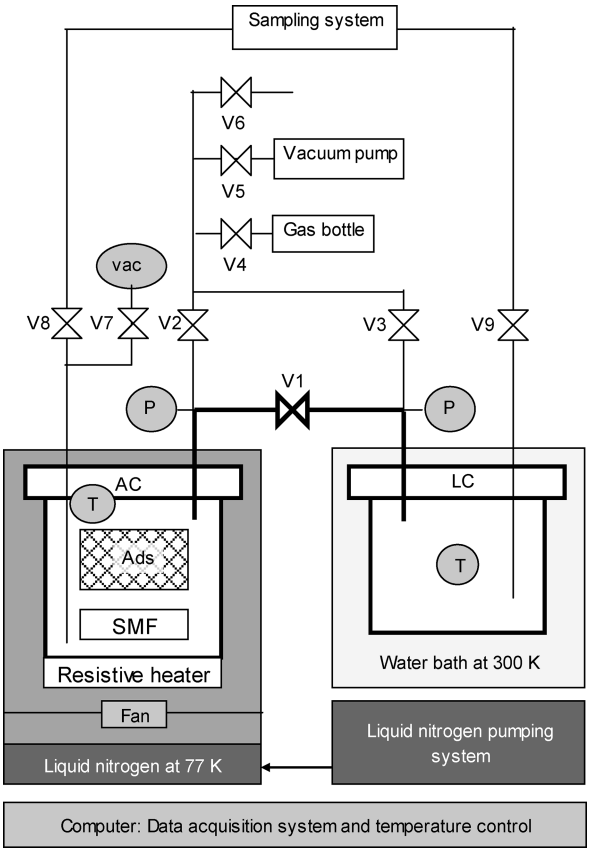

Figure 1. Schematic diagram of the upgraded high pressure volumetric-type apparatus: AC, adsorption cell; LC, loading cell; P, pressure gauge; vac, vacuum gauge; V, actuated valve; T, temperature sensor; Ads, adsorbent holder and adsorbent; SMF, stepper motor fan.

VOLUMETRIC-TYPE APPARATUS FOR MIXTURE ADSORPTION

The high pressure volumetric-type adsorption apparatus consisted of the gas loading cell immersed in a water bath at 300 K and the adsorption cell housed in a cryogenic Dewar, as shown in Figure 1. The two vessels are connected by a gas transfer line with a shutoff valve. Details on the construction and operation of this apparatus, including descriptions of the instruments used for the pressure and temperature measurements, are described in detail in our previous paper.[31] The motivations for changes to the original apparatus included (i) measuring gas mixtures, (ii) reducing the magnitude of temperature gradients in the adsorption cell, and (iii) improving the operability of the apparatus.

A new gas sampling system was added to the apparatus to allow the composition of gas mixtures in the loading cell and the adsorption cell to be measured using a gas chromatograph (Varian CP-3800, with 25 m long × 0.53 mm diameter column of PoroPlot Q packing). A sample loop was connected to the loading and adsorption cells using zero-volume valves (models CSD4UW and C6W, Valco Instruments Co. Inc., USA), and this loop was filled with the gas to be analyzed. The volume of the sample loop could be varied from (0.1 to 8) cm^3 corresponding to the pressure in the adsorption or loading cells, which ranged from (200 to 6500) kPa: the sample loop volume was chosen so that the gas sample could be reduced to a safe pressure for collection in a glass GC syringe (2.5 cm^3). For each measurement

dx.doi.org/10.1021/je200812y |J. Chem. Eng. Data 2012, 57, 93–101

of a gas composition, two samples each filling one syringe were taken from the sample loop, which allowed 10 injections (each of 0.5 cm^3 of gas) into the gas chromatograph (GC). The compositions of the samples were determined with the GC's thermal conductivity detector (TCD).

The procedures used for GC detector calibration and analysis are similar to those described by Kandil et al.[35] For mixtures of CH_4 and CO_2 in the adsorption or loading cell at pressures up to 6500 kPa, the combined relative uncertainty of the measured component mole fractions resulting from the sampling method and detector calibration was less than 4 % of the measured CO_2 mole fraction, which in this work ranged from 0.0001 to 0.1. (The minimum resolvable CO_2 mole fraction was about 10^{-6}.) However, we found that small quantities of air could contaminate the gas in the syringe during transfer to the GC and, consequently, N_2 mole fractions below 0.05 could not be measured reliably. To address this sampling issue we have designed and are constructing an upgraded sampling system with a direct connection to the GC.

To ensure that gas mixtures in contact with the adsorbent were compositionally homogeneous, a cryogenically and vacuum compatible stepper motor (model C17-2, Arun Microelectronics Ltd., England) was used to drive a fan installed beneath the adsorbent holder. This fan forced the circulation of gas inside the adsorption cell and through the adsorbent bed, reducing concentration gradients and temperature gradients in the adsorption cell. In addition, relative to the apparatus previously described,[31] the internal volumes of the adsorption and loading cells were reduced from (700 to 435) cm^3 and from (1800 to 770) cm^3, respectively. This reduction in the ratio of void volume to adsorbent mass results in a lower level of uncertainty in the adsorption measurements, improves the temperature homogeneity in the adsorption cell, and reduces the inventory of high-pressure gas required in the experiment. The volumetric technique for measuring adsorption capacities requires an accurate knowledge of the volumes of the vessels between which gas is being transferred. The calibration procedure using helium and argon to determine the cell volumes with an uncertainty of 0.5 cm^3 was detailed in Watson et al.[31] Pressure tests were regularly conducted to ensure that there were no measurable gas leaks, which can if present affect significantly the calculated adsorption capacities.

In the modified volumetric-type apparatus, several other minor changes were made to improve the integrity and operability of the system. The new features included: bursting discs to protect the expensive pressure and vacuum gauges, actuated valves replaced manual valves in the apparatus manifold to allow remote operation, and a vacuum gauge was added to monitor pressure in the adsorption cell during in situ degassing of the adsorbent. The total volume of the non-temperature controlled lines connecting the adsorption and loading cells was approximately 3 cm^3, which contributed an uncertainty of less than 0.2 % to the measured adsorption capacities.

EXPERIMENTAL PROCEDURES

Prior to the adsorption measurements, the chabazite was regenerated (in a separate cell) under vacuum (1 Pa) at 623 K for 24 h. The mass of the regenerated chabazite loaded into the adsorption cell was m_{ads} = 18.25 ± 0.01 g. Prior to each adsorption isotherm measurement the chabazite was flushed with He and then degassed in situ under vacuum (30 Pa) at 360 K for 48 h; in addition, the loading cell and the manifold were flushed and evacuated several times.

The method for measuring adsorption capacity with the high pressure volumetric-type apparatus is detailed elsewhere.[31] After each gas transfer, equilibrium was considered to be reached when the value of measured adsorption capacity was stable within 0.2 % over one hour. The adsorption kinetics of the natural chabazite were observed to be fast,[33] and three hours at most were required for each pressure step. For pure fluids, the repeatability of the adsorption capacity data along each isotherm (including adsorption and desorption steps) was better than 2 %. These observations indicate that the equilibrium sorption behavior of all three pure gases was completely reversible.

The protocol for gas mixture measurements is similar to that for pure gases. However, before the sorption isotherm for the gas mixture started, the loading cell was filled successively with each of the pure gases comprising the mixture to predetermined pressures. The composition of the resulting gas mixture in the loading cell was estimated by material balance from the measured pressure and temperature and the reference equations of state for CH_4,[36] CO_2,[37] and their mixtures[38] as implemented in the software REFPROP 8.0.[39] The relative uncertainty of the mixture composition determined by this material balance method was 0.4 % of the minor component's mole fraction. The gas compositions in both the loading cell and adsorption cell were measured with the GC at the end of each pressure step, with a relative uncertainty of 4 % in the mole fraction of the minor component. The gas composition measured with the GC was always consistent with that determined by the material balance method.

During a gas mixture measurement, the material balance for each component (index i) in the closed system comprising the adsorption cell + loading cell gives:

$$V_L([y_i\rho(p,T,y)]_L^{initial} - [y_i\rho(p,T,y)]_L^{final}) + V_A([y_i\rho(p,T,y)]_A^{initial} - [y_i\rho(p,T,y)]_A^{final}) + (n_{ads,i}^{initial} - n_{ads,i}^{final}) = 0 \quad (1)$$

Here the subscripts L and A denote the loading and adsorption cells, respectively; the superscripts "initial" and "final" denote conditions before and after the transfer of fluid between the cells; p, T, and V are the pressure, temperature, and volume of fluid in the cell; y_i is the mole fraction of the component i in the gas phase (y is the mixture composition array); and $n_{ads,i}$ is the number of moles of component i adsorbed. The molar density of the gas mixture ρ was determined at the measured pressure, temperature, and composition, from the GERG-2004 EOS[38] as implemented in the software REFPROP 8.0.[39] For both pure fluids and mixtures, the uncertainty in the adsorption measurement was dominated by the uncertainty of the temperature measurements in adsorption cell. We have designed and are constructing an upgraded volumetric-type apparatus with a better temperature control and measurement system for the adsorption cell.

Implicit in the use of eq 1 is the assumption that the fluid densities are uniform throughout each of the two volumes V_A and V_L. In practice, if $T_A \neq T_L$ then a density gradient will necessarily exist somewhere in the lines connecting the adsorption and loading cells, and the assumption is violated to some degree. The impact of this, however, is largely mitigated by the process of volume calibration as long as the variation in molar density of the calibration fluid (helium) is similar to that of the adsorbate fluid. Particular care must thus be taken when transferring condensable fluids such as CO_2 at pressures close to saturation, because if a

Table 1. Adsorption Capacities for Pure N_2, CO_2, and CH_4 on Chabazite: Excess Adsorption Q_{ex}, Absolute Adsorption Q_{abs}, and the Corresponding Uncertainty $u(Q_{abs})$

T	p	Q_{ex}	Q_{abs}	$u(Q_{abs})$
K	kPa	mmol·g^{-1}	mmol·g^{-1}	mmol·g^{-1}
		N_2		
304.6	62.9	0.27	0.27	0.02
304.6	196.1	0.63	0.64	0.02
304.6	583.9	1.14	1.15	0.05
304.5	1994.0	1.76	1.82	0.15
304.5	3012.6	1.99	2.09	0.24
304.6	1106.3	1.46	1.48	0.21
304.5	420.1	0.97	0.98	0.08
304.5	175.7	0.59	0.59	0.03
244.2	5.9	0.23	0.23	0.01
244.1	19.2	0.55	0.55	0.01
244.1	71.6	1.11	1.11	0.01
244.2	2031.9	2.58	2.69	0.22
244.2	3004.2	2.67	2.85	0.37
244.2	1301.2	2.41	2.47	0.33
244.2	562.3	2.03	2.06	0.14
244.2	253.5	1.66	1.67	0.06
244.1	122.9	1.32	1.32	0.03
244.1	69.3	1.06	1.06	0.02
		CH_4		
244.1	78.9	0.65	0.65	0.01
244.0	193.2	1.01	1.01	0.02
244.0	395.8	1.29	1.30	0.03
244.1	2089.4	1.96	2.04	0.16
244.1	3036.0	2.14	2.27	0.26
244.4	1135.3	1.69	1.73	0.22
244.7	425.7	1.30	1.31	0.08
244.5	4.1	0.45	0.45	0.01
244.1	15.3	0.94	0.94	0.01
304.5	70.1	1.48	1.48	0.01
304.5	1944.8	2.77	2.90	0.22
304.5	2972.5	2.86	3.08	0.40
304.5	1399.5	2.73	2.82	0.36
304.4	616.8	2.40	2.43	0.16
304.5	271.9	2.02	2.03	0.07
304.5	122.0	1.69	1.69	0.03
		CO_2		
304.6	5.8	2.37	2.37	0.02
304.6	98.5	3.27	3.27	0.02
304.6	244.0	3.56	3.57	0.02
304.6	757.2	3.95	4.00	0.06
304.6	1961.0	4.39	4.56	0.17
304.6	2995.1	4.77	5.09	0.29
304.6	1209.5	4.32	4.42	0.24
304.6	471.2	3.98	4.02	0.09
304.6	188.9	3.70	3.72	0.03

liquid phase forms in the connecting lines a significant error could be introduced into the material balance calculation.

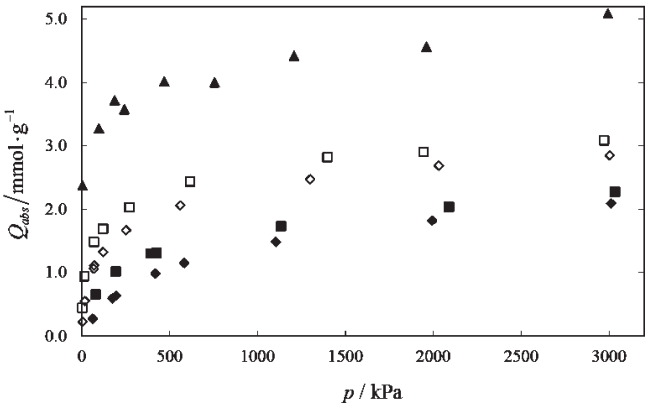

Figure 2. Pure fluid isothermal adsorption capacities measured in this work. ♦, N_2 at 305 K; ◇, N_2 at 244 K; ■, CH_4 at 305 K; □, CH_4 at 244 K; and ▲, CO_2 at 305 K.

To avoid condensation in the connecting lines when conducting volumetric-type adsorption experiments with CO_2, one approach is to control the temperature of the lines as done, for example, by He et al.[40] The alternative approach is to ensure that the maximum operating pressure is significantly below the saturation pressure corresponding to the coldest temperature anywhere in the apparatus. Watson et al.[31] followed this second approach successfully, and it was also adopted for this work. The maximum CO_2 pressure in the system was maintained at least 400 kPa below the saturation pressure corresponding to the lowest temperature in the apparatus.

The component excess adsorption capacities $Q_{ex,i}$ were calculated from the $(\Delta n_{ads,i})_j \equiv (n_{ads,i}^{final} - n_{ads,i}^{initial})_j$, using the method described by Watson et al.,[31] where the index j enumerates the transfers between the loading and adsorption cells. To convert the excess adsorption capacity $Q_{ex,i}$ to the absolute adsorption capacity $Q_{abs,i}$, the density of the adsorbed phase mixture was estimated using an ideal mixing rule and the density of the adsorbed phase for pure compounds, which can be estimated using a variety of methods with a scatter of about 10 %.[41] The uncertainty of the absolute adsorption capacity $u(Q_{abs,i})$ was then estimated from an error propagation analysis.

PURE GAS ADSORPTION RESULTS

Data for the pure gas adsorption isotherms of N_2 and CH_4 on chabazite at (244 and 305) K for pressures from (5 to 3000) kPa are reported in Table 1, together with the CO_2 adsorption data measured at 305 K. These data are also presented graphically in Figure 2; the shape of each of these isotherms corresponds to Type I in the IUPAC classification.[42] As discussed below, the adsorption data for pure CO_2 measured at 244 K were found to be unreliable, most likely due to inadequate degassing.

For the pure fluid adsorption isotherms, a least-squares regression analysis was used to determine the best-fit parameters of the Toth model[43] by minimizing the standard deviation (SD = $((1/N)\Sigma(Q_{abs}^{meas} - Q_{abs}^{calc})^2)^{1/2}$, N being the number of data points regressed):

$$Q_{abs}^{calc} = Q_{max}\frac{Kp}{(1 + (Kp)^n)^{1/n}} \quad (2a)$$

$$K = K_0 \exp\left(\frac{-\Delta H}{RT}\right) \quad (2b)$$

dx.doi.org/10.1021/je200812y |J. Chem. Eng. Data 2012, 57, 93–101

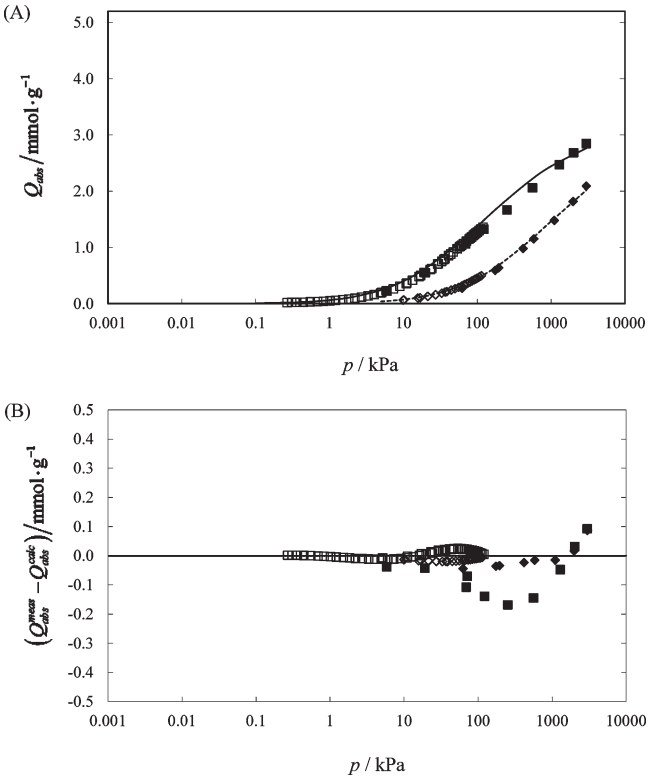

Figure 3. Measured and modeled N_2 adsorption capacities for the natural chabazite. (A) Absolute adsorption capacities. ♦, this work at 305 K; ■, this work at 244 K; ◇, Jensen et al.[33] at 302 K; □, Jensen et al.[33] at 248 K. The lines represent the predictions of the Toth model (eq 2) fitted to the "Overall" data set: calculated capacities at 305 K are indicated with a dashed line, while calculated capacities at 244 K are indicated with a solid line. (B) Deviations between the measured and the calculated capacities.

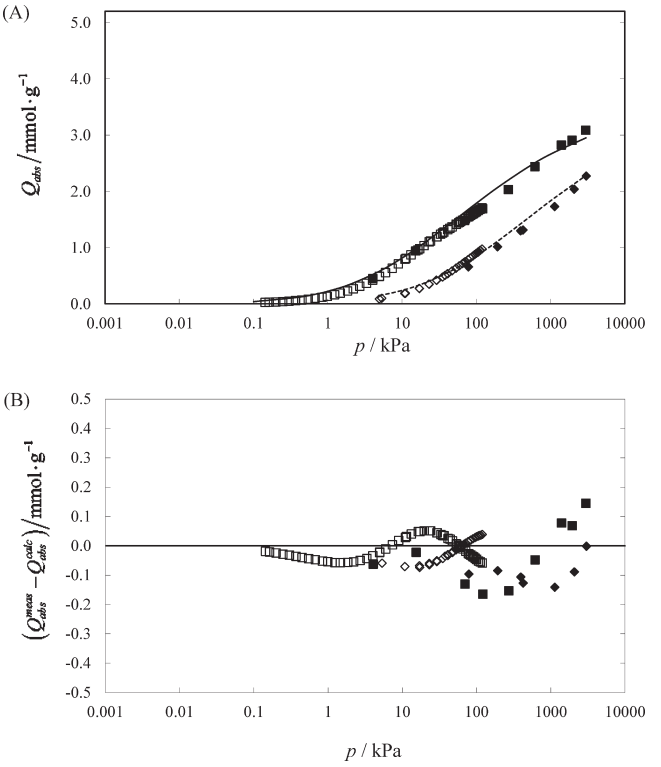

Figure 4. Measured and modeled CH_4 adsorption capacities for the natural chabazite. (A) Absolute adsorption capacities. ♦, this work at 305 K; ■, this work at 244 K; ◇, Jensen et al.[33] at 302 K; □, Jensen et al.[33] at 248 K. The lines represent the predictions of the Toth model (eq 2) fitted to the Overall data set: calculated capacities at 305 K are indicated with a dashed line while calculated capacities at 244 K are indicated with a solid line. (B) Deviations between the measured and the calculated capacities.

Here R is the molar gas constant, and ΔH is the isosteric enthalpy of adsorption at zero coverage. In the regression, ΔH was treated as an adjustable parameter along with the three empirical parameters Q_{max}, K_0, and n. The model is adequate for the purpose of engineering design calculations. It contains only four parameters, and it provides an analytical expression for the Q_{abs} that is an explicit function of temperature and pressure.

To assess the accuracy of the high-pressure volumetric measurements, we compared these results to adsorption data obtained for the same batch of chabazite at lower pressures from (0.001 to 120) kPa using a commercial sorption system (ASAP2020).[33] The comparison of pure gas isotherms obtained with the high-pressure volumetric system and the low-pressure ASAP2020 are shown in Figures 3A to 5A. The deviations between the measured data and the predictions of the Toth equations are shown in Figures 3B to 5B. Apart from the CO_2 isotherm measured at 244 K, the adsorption data at 100 kPa collected on the high-pressure apparatus were within 10 % of the adsorption capacities measured on the commercial ASAP2020 system. The CO_2 adsorption data measured at 244 K with the high-pressure apparatus were inconsistent with the high-pressure measurements at 305 K and with the measurements made at 248 K with the ASAP2020 system, as indicated by the approximate location of these data in Figure 5A. We attribute this inconsistency to improper degassing of the sample prior to this measurement; we are confident that it was not caused by CO_2 condensation despite our precautions because such a systematic error would result in apparent adsorption capacities greater than expected, whereas the apparent capacities observed at 244 K were smaller than measured at 305 K. These data have been omitted from Table 1 and from the data sets used for fitting the Toth equation. This problem was only discovered several weeks after the chabazite measurements were completed and when the system was being used to measure other adsorbents. However the low-pressure CO_2 data measured with the ASAP2020 system at 244 K were available and are sufficient to explain the high-pressure adsorption data measured for the $CH_4 + CO_2$ mixture at this temperature. This example highlights the importance of proper sample preparation in adsorption measurements and the importance of rapid data analysis following its acquisition.

For each pure gas, the four-parameter Toth model in eq 2 was regressed to three sets of adsorption data: the low pressure isotherms collected with the ASAP2020 (LowP),[33] the high pressure isotherms collected in the current work (HighP), and a combined data set for pressures from (0.001 to 3000) kPa collected with the two apparatus (Overall). The optimized parameter values resulting from the regression of eq 2 to the Overall data set are shown in Table 2 together with their statistical uncertainties. The fits to the other data sets were conducted to quantify the errors associated with extrapolating adsorption capacity models outside the range of the data to which

dx.doi.org/10.1021/je200812y |J. Chem. Eng. Data 2012, 57, 93–101

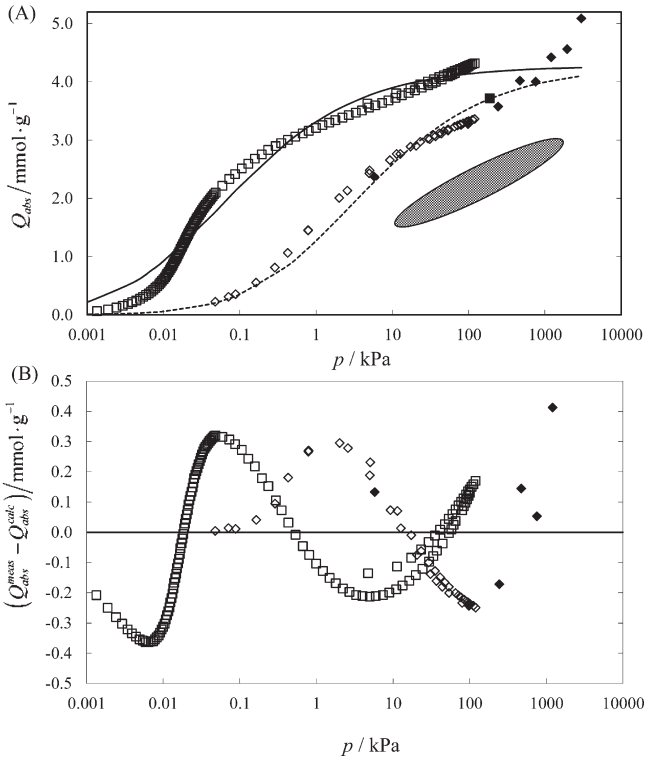

Figure 5. Measured and modeled CO_2 adsorption capacities for the natural chabazite. (A) Absolute adsorption capacities. ♦, this work at 305 K; ◇, Jensen et al.[33] at 302 K; □, Jensen et al.[33] at 248 K. The lines represent the predictions of the Toth model (eq 2) fitted to the Overall data set: calculated capacities at 305 K are indicated with a dashed line, while calculated capacities at 244 K are indicated with a solid line. The ellipse in (A) shows the approximate location of our CO_2 isotherm at 244 K which was clearly inconsistent with the other measurement. These data were not used for the Toth equation fitting. (B) Deviations between the measured and the calculated capacities.

Table 2. Parameters of the Toth Models (eq 2) Fitted to the Adsorption Capacities for Each Pure Gas Using the Overall Data from This Work and Jensen et al.[33] from (244 to 305) K[a]

gas	N_2	CH_4	CO_2
no. of data	152	155	219
Q_{max}/mmol·g^{-1}	3.24 ± 0.05	3.60 ± 0.09	4.27 ± 0.05
$K_0 \cdot 10^6$/kPa^{-1}	0.51 ± 0.05	2.48 ± 0.39	0.035 ± 0.022
$-\Delta H$/kJ·mol^{-1}	21.8 ± 0.2	22.5 ± 0.4	44.9 ± 1.1
n	0.56 ± 0.01	0.40 ± 0.01	0.46 ± 0.02
SD/mmol·g^{-1}	0.03	0.05	0.19
AARD	5 %	11 %	20 %

[a] SD is the standard deviation (SD = $((1/N)\Sigma(Q_{abs}^{meas} - Q_{abs}^{calc})^2)^{1/2}$), and AARD is the absolute average relative deviation (AARD = $(1/N)\Sigma(|Q_{abs}^{meas} - Q_{abs}^{calc}|)/(Q_{abs}^{meas})$), N being the number of data points regressed.

they were fit. In the case of N_2 for example, the Overall data set has a standard deviation (SD) of 0.03 mmol·g^{-1} from the "Overall" Toth model. A model regressed only to the LowP data set has a SD of 0.004 mmol·g^{-1}; however when that model is extrapolated to the high pressure range, the SD from the high pressure data is 0.09 mmol·g^{-1}. Moreover, the values of the best fit parameters, Q_{max}, K_0, and n, obtained by fitting to the LowP data set for N_2 each differ from those obtained by fitting to the HighP data set by between 50 % and 300 %, all well beyond their estimated statistical uncertainties. Similar results were obtained by fitting to the different subranges of the CH_4 data. For example the measured adsorption capacity of CH_4 at 3000 kPa and 244 K was 3.1 mmol·g^{-1}, while the Toth models regressed to the LowP data and Overall data predicted (2.0 and 2.9) mmol·g^{-1}, respectively. These numerical experiments indicate the potential pitfalls of using low-pressure adsorption measurements to predict high-pressure adsorption capacities, and vice versa. The latter case is particularly relevant when predicting component sorption capacities for gas mixtures when the partial pressure of one component is very low.

The results of such numerical experiments are less conclusive with the CO_2 data, primarily because the CO_2 adsorption isotherms have an unusual shape, when plotted on a log scale, in comparison with the corresponding N_2 and CH_4 adsorption isotherm shapes. There is relatively strong adsorption for CO_2 at very low pressures, and the isosteric enthalpy of adsorption at zero coverage determined from regression of the Toth model to the CO_2 data is about −45 kJ·mol^{-1}, which is more than twice that for the N_2 and CH_4 cases. Such adsorption behavior has been observed by others with chabazite or other zeolites[20,26,27] and is due to the specific interactions of the quadrupole of the CO_2 molecule with the electrical field created by the cations that make up the zeolite's structure. Ridha and Webley[27] showed that the isothermal adsorption capacity of CO_2 on chabazites exhibited unusual, nonlinear trends at pressure ranging from (0.001 to 1) kPa, and consequently, the determination of the Henry's constants was problematic. In this work, the quality of the Toth model fit to the CO_2 data was worse than for the CH_4 and N_2 cases, with a SD of 0.19 mmol·g^{-1} and a maximum deviation of 0.4 mmol·g^{-1}; these deviations are larger than the estimated experimental uncertainty. The CO_2 isotherm data were also regressed using other standard equilibrium capacity models; however, no improvement over the Toth model was found.

The two most important adsorbent properties for gas separation applications are capacity and selectivity. An adsorbent's equilibrium selectivity, α_{ij}, for two components in a gas mixture (i is the more adsorbed component and j the less adsorbed component) is defined (for example, Saha et al.[44]):

$$\alpha_{ij} \equiv \left(\frac{x_i}{x_j}\right)\left(\frac{y_j}{y_i}\right) \xrightarrow[y_j = y_i]{} \alpha_{ij} = \left(\frac{Q_{\mathrm{abs},i}}{Q_{\mathrm{abs},j}}\right) \quad (3)$$

Here, y and x are the mole fractions of a component in the vapor and adsorbed phases, respectively, and the second equality holds in the case of an equimolar mixture. Estimates of an adsorbent's equilibrium selectivity are frequently made on the basis measured pure fluid capacities. For example, Gu and Lodge[45] and Jensen et al.[33] estimated so-called "inferred" or "ideal" selectivities which are computationally simple to evaluate but do not account for competition between species for adsorption sites. More rigorous predictions of mixture selectivity can be made by using the ideal adsorbed solution (IAS) theory developed by Myers and Prausnitz;[46] however, mixture measurements will still ultimately be required if an adsorbent is to be adopted for a gas separation application. Equilibrium selectivities estimated from the pure fluid measurements of the chabazite indicate that while it is unlikely to be suitable for separating CH_4 and N_2 it may have potential for removing CO_2 from natural gas. Adsorption data for

Table 3. Equilibrium Vapor Compositions, Adsorption Capacities, and Selectivities for CH_4 + CO_2 Mixtures at (244 and 305) K, at Total Pressures from (370 to 2800) kPa

gas phase measurement				adsorbed phase measurement						
				CH_4			CO_2			
T	p total			Q_{exc}	Q_{abs}	$u(Q_{abs})$	Q_{exc}	Q_{abs}	$u(Q_{abs})$	selectivity
K	kPa	$10^6 \cdot y_{CO_2}$	$10^6 \cdot u(y_{CO_2})$	mmol·g^{-1}	mmol·g^{-1}	mmol·g^{-1}	mmol·g^{-1}	mmol·g^{-1}	mmol·g^{-1}	α_{CO_2,CH_4}
304.5	639.9	670	31	1.36	1.37	0.13	0.36	0.36	0.02	392
304.5	1184.1	842	36	1.49	1.52	0.14	0.62	0.63	0.01	492
304.4	1734.2	1126	46	1.54	1.59	0.17	0.87	0.90	0.01	502
304.4	2209.6	1528	57	1.51	1.57	0.20	1.09	1.14	0.01	474
304.4	2743.8	2298	72	1.44	1.52	0.25	1.33	1.40	0.01	400
304.4	1770.4	2358	72	1.29	1.33	0.22	1.32	1.36	0.01	433
304.5	1004.2	2942	90	1.09	1.11	0.13	1.31	1.34	0.01	409
304.5	374.9	4727	148	0.93	0.93	0.07	1.30	1.31	0.01	297
244.0	622.6	123	11	2.08	2.11	0.14	0.44	0.44	0.01	1700
244.0	989.9	153	10	2.11	2.16	0.16	0.66	0.67	0.01	2030
244.0	1510.7	215	7	1.99	2.06	0.21	0.96	1.00	0.01	2260
244.0	1998.9	229	11	1.81	1.90	0.28	1.26	1.32	0.01	3030
244.0	2552.2	257	12	1.54	1.65	0.35	1.61	1.72	0.01	4060
244.1	1991.3	241	11	1.54	1.62	0.35	1.61	1.68	0.01	4300
244.1	1291.2	258	8	1.62	1.67	0.25	1.60	1.60	0.01	3710
244.0	1003.2	264	9	1.57	1.61	0.17	1.60	1.60	0.01	3760
244.1	448.8	332	12	1.57	1.59	0.11	1.60	1.60	0.01	3030

CO_2 + CH_4 mixtures were therefore acquired and compared with the behavior predicted using the IAS model.

GAS MIXTURE ADSORPTION RESULTS

We measured adsorption capacities at (244 and 305) K at total pressures from (370 to 2800) kPa for mixtures of CH_4 + CO_2. For each isotherm, the mixture transferred from the loading cell to the adsorption cell had a composition of approximately $0.95CH_4$ + $0.05CO_2$. For desorption steps, the loading cell was evacuated, and the vapor phase in equilibrium with the adsorbed phase was transferred out of the adsorption cell. In Table 3 the measured composition of the equilibrium vapor phase is listed together with the excess and absolute adsorption capacities determined for each component. The estimated uncertainties in the vapor composition and adsorption capacities of each component are also included in Table 3. At equilibrium, the CO_2 mole fraction of the vapor was reduced to about 0.0013 and 0.0002 at (305 and 244) K, respectively. The equilibrium selectivities α_{CO_2,CH_4} measured at each condition are also listed in Table 3 and had average values over all the data points of 420 and 3100 at (305 and 244) K, respectively.

Figure 6 shows the component adsorption capacities measured for the binary mixture as a function of the total pressure at (244 and 305) K. Systems with two sorbates have three degrees of freedom,[46] and the volumetric method employed in this work does not permit control of the equilibrium vapor-phase composition. For this reason, only data measured along an adsorption pathway (increasing pressure) are shown in Figure 6. The predictions of the ideal adsorbed solution (IAS) theory[46] implemented using the algorithm of Valenzuela and Myers[47] are also shown in Figure 6. The IAS theory is a fully predictive model for gas mixture adsorption based only on the knowledge of the pure fluid adsorption isotherms. In this case the predictions of the adsorbed CH_4 capacities are consistent with the measured values within the experimental uncertainties—this agreement was achieved with no parameter adjustments. The IAS predictions for the CO_2 capacities at equilibrium do not show quite the same level of consistency within the estimated experimental uncertainties: the IAS predictions are on average 0.3 mmol·g^{-1} lower than the measured values at 305 K and 0.2 mmol·g^{-1} greater than the measured values at 244 K. Activity coefficients for the adsorbed phase's CO_2 component could be used to force the model and the data to agree. However, the predictions of the IAS model are sensitive to the uncertainty of the pure fluid adsorption isotherms, which would propagate into any activity coefficient determination.

For example, consider a (worst-case) scenario in which the Toth models used to describe the pure component adsorption on the chabazite were fit to the HighP data for CO_2 and the LowP data[33] for CH_4. The resulting IAS predictions for Q_{abs,CO_2} and Q_{abs,CH_4} would shift by an average of (+0.1 and −0.5) mmol·g^{-1}, respectively, at 305 K and (+0.6 and −1.0) mmol·g^{-1}, respectively, at 244 K. As a consequence of these shifts, the IAS model would predict an inversion of the most adsorbed component from CH_4 to CO_2 above 2300 kPa at 305 K, and above 800 kPa at 244 K. This further illustrates the importance of measuring adsorption data for pure fluids over a wide range of pressures and using such data in the determination of model adsorption isotherms by regression.

The measured adsorption data for the CH_4 + CO_2 mixtures confirm that the chabazite has significant potential for removing CO_2 from natural gas, particularly at low temperatures and high pressures. Furthermore, the IAS predictions were shown to be reasonably consistent with the mixture measurements, indicating

dx.doi.org/10.1021/je200812y |J. Chem. Eng. Data 2012, 57, 93–101

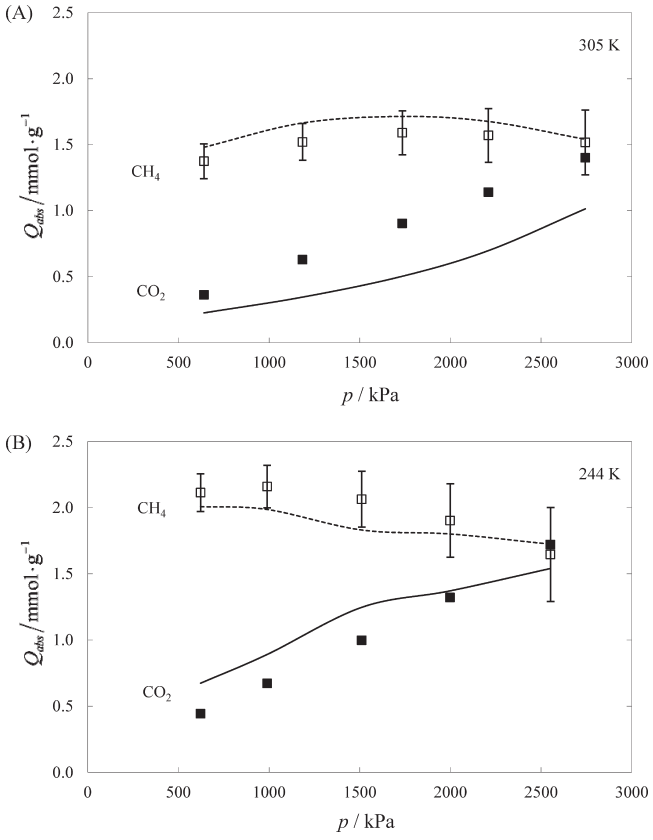

Figure 6. Absolute adsorption capacities measured for each component of the CO_2 + CH_4 mixture as a function of the mixture's total pressure, at 305 K (A) and 244 K (B): ■, CO_2; and □, CH_4. The lines are the capacities predicted with the IAS model (dashed for CH_4 and solid for CO_2) using the Toth model (eq 2) regressed to the Overall data set obtained in this work and by Jensen et al.[33]

that the adsorption behavior can be modeled reliably over the range of conditions likely to be explored in the design of a separation process. Of course, the affinity of zeolites for CO_2 is well-known, and they are already used commercially to reduce the CO_2 content of natural gas to LNG production specifications.[48] However, this work demonstrates that by exploring lower temperatures significant capacity and selectivity gains are achievable. With appropriate integration of such a low temperature PSA process into a cryogenic processing plant, it may be possible to treat more gas for the same cost or, alternatively, the same amount of gas at reduced cost.

AUTHOR INFORMATION

Corresponding Author

*E-mail: eric.may@uwa.edu.au.

Funding Sources

The research was funded by Chevron Energy Technology Company, the Western Australian Energy Research Alliance, and the Australian Research Council.

ACKNOWLEDGMENT

The authors thank Craig Grimm and Paul Hofman for helping to construct the apparatus, Dr. Brendan Graham for his guidance with the GC measurements, and Wagish Deshpande and Arnout van Lent for their assistance with the measurements and the modeling.

REFERENCES

(1) *Key world energy statistics*; International Energy Agency: Paris, 2010; p 78.

(2) Kindlay, A. J.; Parrish, W. R. *Fundamentals of Natural Gas Processing*; CRC Press: Boca Raton, FL, 2006.

(3) Tagliabue, M.; Farrusseng, D.; Valencia, S.; Aguado, S.; Ravon, U.; Rizzo, C.; Corma, A.; Mirodatos, C. Natural gas treating by selective adsorption: Material science and chemical engineering interplay. *Chem.—Eng. J.* **2009**, *155*, 553–566.

(4) Hale, P.; Lokhandwala, K. In *Advances in membrane materials provide new solutions in the gas business*. Laurance Reid Gas Conditioning Conference Proceedings, Norman, OK, 2004.

(5) Yang, R. T. *Gas Separation by Adsorption Processes*; Butterworth: Stoneham, MA, 1987; p 352.

(6) Ruthven, D. M.; Farooq, S.; Knaebel, K. S. *Pressure Swing Adsorption*. Wiley-VCH: New York, 1994.

(7) Habgood, H. W. The kinetics of molecular sieves action. Adsorption of nitrogen-methane mixtures by Linde Molecular Sieve 4A. *Can. J. Chem.* **1958**, *36*, 1384–1397.

(8) Habgood, H. W. Removal of nitrogen from natural gas. U.S. Patent 2,843,219, 1958.

(9) Lederman, P. B.; Williams, B. The adsorption of nitrogen-methane on molecular sieve. *AIChE J.* **1964**, *10*, 30–34.

(10) Cansado, I. P. P.; Maurão, P. A. M.; Ribeiro Carrott, M. L.; Carrott, P. J. M. Activated Carbons Prepared from Natural and Synthetic Raw Materials with Potential Applications in Gas Separations. *Adv. Mater. Res.* **2010**, *107*, 1–7.

(11) Esteves, I. A. A. C.; Lopes, M. S. S.; Nunes, P. M. C.; Mota, J. P. B. Adsorption of natural gas and biogas components on activated carbon. *Sep. Purif. Technol.* **2008**, *62*, 281–296.

(12) Sircar, S. Gas Separation and Storage by Activated Carbons. In *Adsorption by Carbons*, Bottani, E. J., Tascón, J. M. D., Eds.; Elsevier: Amsterdam, 2008; pp 565−592.

(13) Beutekamp, S.; Harting, P. Experimental Determination and Analysis of High Pressure Adsorption Data for Pure Gases and Gas Mixtures. *Adsorption* **2002**, *8*, 255–269.

(14) Bae, Y.-S.; Lee, C.-H. Sorption kinetics of eight gases on a carbon molecular sieve at elevated pressure. *Carbon* **2005**, *43*, 95–107.

(15) Cavenati, S.; Grande, C. A.; Rodrigues, A. Separation of Methane and Nitrogen by Adsorption on Carbon Molecular Sieve. *Sep. Sci. Technol.* **2005**, *40*, 2721–2743.

(16) Cavenati, S.; Grande, C. A.; Rodrigues, A. E. Upgrade of methane from landfill gas by pressure swing adsorption. *Energy Fuels* **2005**, *19*, 2545–2555.

(17) Guest, J. E.; Williams, C. D. Efficient methane/nitrogen separation with low-sodium clinoptilolite. *Chem.—Eng. J.* **2002**, *23*, 2870–2871.

(18) Jayaraman, A.; Hernández-Maldonado, A. J.; Yang, R. T.; Chinn, D.; Munson, C. L.; Mohr, D. H. Clinoptilolites for nitrogen/methane separation. *Chem. Eng. Sci.* **2004**, *59*, 2407–2417.

(19) Delgado, J.; Uguina, M. A.; Gómez, J. M.; Ortega, L. Adsorption equilibrium of carbon dioxide, methane and nitrogen onto Na- and H-mordenite at high pressures. *Sep. Purif. Technol.* **2006**, *48*, 223–228.

(20) Hernandez-Huesca, R.; Diaz, L.; Aguilar-Armenta, G. Adsorption equilibria and kinetics of CO_2, CH_4 and N_2 in natural zeolites. *Sep. Purif. Technol.* **1999**, *15*, 163–173.

(21) Ackley, M. W.; Rege, S. U.; Saxena, H. Application of natural zeolites in the purification and separation of gases. *Microporous Mesoporous Mater.* **2003**, *61*, 25–42.

(22) Faghihian, H.; Pirouzi, M. Nitrogen separation from natural gas by modified clinoptilolite. *Clay Miner.* **2009**, *44*, 289–292.

(23) Alonso-Vicario, A.; Ochoa-Gómez, J. R.; Gil-Río, S.; Gómez-Jiménez-Aberasturi, O.; Ramírez-López, C. A.; Torrecilla-Soria, J.;

Domínguez, A. Purification and upgrading of biogas by pressure swing adsorption on synthetic and natural zeolites. *Microporous Mesoporous Mater.* **2010**, *134*, 100–107.

(24) Breck, D. W. *Zeolite Molecular Sieves*; John Wiley & Sons: New York, 1974.

(25) Singh, R. K.; Webley, P. A. Adsorption of N_2, O_2, and Ar in Potassium Chabazite. *Adsorption* **2005**, *11*, 173–177.

(26) Zhang, J.; Singh, R.; Webley, P. A. Alkali and alkaline-earth cation exchanged chabazite zeolites for adsorption based CO_2 capture. *Microporous Mesoporous Mater.* **2008**, *111*, 478–487.

(27) Ridha, F. N.; Webley, P. A. Anomalous Henry's law behavior of nitrogen and carbon dioxide adsorption on alkali-exchanged chabazite zeolites. *Sep. Purif. Technol.* **2009**, *67*, 336–343.

(28) Coe, C. G.; Roberts, D. A. Process for the purification of permanent gases using chabazite adsorbents. U.S. Patent 4,732,584, 1988.

(29) Coe, C. G.; Gaffney, T. R. Process for the purification of bulk gases using chabazite adsorbents. U.S. Patent 4,943,304, 1990.

(30) Coe, C. G.; Gaffney, T. R.; Srinivasan, R. S. Chabazite for gas separation. U.S. Patent 4,925,460, 1990.

(31) Watson, G.; May, E. F.; Graham, B. F.; Trebble, M. A.; Trengove, R. D.; Chan, K. I. Equilibrium Adsorption Measurements of Pure Nitrogen, Carbon Dioxide, and Methane on a Carbon Molecular Sieve at Cryogenic Temperatures and High Pressures. *J. Chem. Eng. Data* **2009**, *54*, 2701–2707.

(32) Kuznicki, S. M.; Lin, C. C. H.; Bian, J.; Anson, A. Chemical upgrading of sedimentary Na-Chabazite from Bowie, Arizona. *Clays Clay Miner.* **2007**, *55*, 235–238.

(33) Jensen, N. K.; Rufford, T. E.; Watson, G.; Zhang, D. K.; Chan, K. I.; May, E. F. Screening of several zeolites for gas separation applications involving methane, nitrogen, and carbon dioxide. *J. Chem. Eng. Data* **2011**, DOI: DOI: 10.1021/je200817w.

(34) http://www.micromeritics.com/Product-Showcase/ASAP-2020-Physisorption.aspx (accessed July 19, 2011).

(35) Kandil, M. E.; May, E. F.; Graham, B. F.; March, K. N.; Trebble, M. A.; Trengove, R. D.; Huang, S. H. Vapor-liquid equilibria measurements of methane + 2-methylpropane (isobutane) at temperatures from (150 to 250) K and pressures to 9 MPa. *J. Chem. Eng. Data* **2010**, *55*, 2725–2731.

(36) Setzmann, U.; Wagner, W. A New Equation of State and Tables of Thermodynamic Properties for Methane Covering the Range from the Melting Line to 625 K at Pressures up to 100 MPa. *J. Phys. Chem. Ref. Data* **1991**, *20*, 1061–1151.

(37) Span, R.; Wagner, W. A New Equation of State for Carbon Dioxide Covering the Fluid Region from the Triple−Point Temperature to 1100 K at Pressures up to 800 MPa. *J. Phys. Chem. Ref. Data* **1996**, *25*, 1509–1596.

(38) Kunz, O.; Klimeck, R.; Wagner, W.; Jaeschke, M. *The GERG-2004 Wide-Range Reference Equation of State for Natural Gases and Other Mixtures. GERG Technical Monograph*; Fortschr.-Ber. VDI, VDI-Verlag: Düsseldorf, Germany, 2006.

(39) Lemmon, E. W.; Huber, M. L.; McLinden, M. O. *REFPROP−Reference Fluid Thermodynamic and Transport Properties, NIST Standard Reference Database 23*, 8.0; NIST: Gaithersburg, MD, 2007.

(40) He, J.; Shi, Y.; Ahn, S.; Kang, J. W.; Lee, C.-H. Adsorption and Desorption of CO_2 on Korean Coal under Subcritical to Supercritical Conditions. *J. Phys. Chem. B* **2010**, *114*, 4854–4861.

(41) Sudibandriyo, M.; Pan, Z.; Fitzgerald, J. E.; Robinson, R. L.; Gasem, K. A. M. Adsorption of Methane, Nitrogen, Carbon Dioxide, and Their Binary Mixtures on Dry Activated Carbon at 318.2 K and Pressures up to 13.6 MPa. *Langmuir* **2003**, *19*, 5323–5331.

(42) Brunauer, S.; Deming, L. S.; Deming, W. E.; Teller, E. Theory of the Van der Waals adsorption of gases. *J. Am. Chem. Soc.* **1940**, *62*, 1723–1732.

(43) Toth, J. State of equations of the solid-gas interface layers. *Acta Chim. Acad. Sci. Hung.* **1971**, *69*, 311–328.

(44) Saha, D.; Bao, Z.; Jia, F.; Deng, S. Adsorption of CO_2, CH_4, N_2O, and N_2 on MOF-5, MOF-177, and zeolite 5A. *Environ. Sci. Technol.* **2010**, *44*, 1820–1826.

(45) Gu, Y.; Lodge, T. P. Synthesis and Gas Separation Performance of Triblock Copolymer Ion Gels with a Polymerized Ionic Liquid Mid-Block. *Macromolecules* **2011**, *44*, 1732–1736.

(46) Myers, A. L.; Prausnitz, J. M. Thermodynamics of mixed-gas adsorption. *AIChE J.* **1965**, *11*, 121–127.

(47) Valenzuela, D. P.; Myers, A. L. *Adsorption equilibrium data handbook*; Prentice Hall: Upper Saddle River, 1989; p 364.

(48) UOP Contaminant removal from Natural Gas Streams. http://www.uop.com/products/adsorbents/natural-gas/#natural-gas-adsorbents (accessed 19 July 2011).